Observation of enhancement of charmed baryon-to-meson ratio in Au+Au collisions at $\sqrt{s_{\rm NN}} = 200\,\rm GeV$

J. Adam,[6] L. Adamczyk,[2] J. R. Adams,[39] J. K. Adkins,[30] G. Agakishiev,[28] M. M. Aggarwal,[40] Z. Ahammed,[59] I. Alekseev,[3,35] D. M. Anderson,[53] A. Aparin,[28] E. C. Aschenauer,[6] M. U. Ashraf,[11] F. G. Atetalla,[29] A. Attri,[40] G. S. Averichev,[28] V. Bairathi,[22] K. Barish,[10] A. Behera,[51] R. Bellwied,[20] A. Bhasin,[27] J. Bielcik,[14] J. Bielcikova,[38] L. C. Bland,[6] I. G. Bordyuzhin,[3] J. D. Brandenburg,[48,6] A. V. Brandin,[35] J. Butterworth,[44] H. Caines,[62] M. Calderón de la Barca Sánchez,[8] D. Cebra,[8] I. Chakaberia,[29,6] P. Chaloupka,[14] B. K. Chan,[9] F-H. Chang,[37] Z. Chang,[6] N. Chankova-Bunzarova,[28] A. Chatterjee,[11] D. Chen,[10] J. H. Chen,[18] X. Chen,[47] Z. Chen,[48] J. Cheng,[55] M. Cherney,[13] M. Chevalier,[10] S. Choudhury,[18] W. Christie,[6] H. J. Crawford,[7] M. Csanád,[16] M. Daugherity,[1] T. G. Dedovich,[28] I. M. Deppner,[19] A. A. Derevschikov,[42] L. Didenko,[6] X. Dong,[31] J. L. Drachenberg,[1] J. C. Dunlop,[6] T. Edmonds,[43] N. Elsey,[61] J. Engelage,[7] G. Eppley,[44] R. Esha,[51] S. Esumi,[56] O. Evdokimov,[12] J. Ewigleben,[32] O. Eyser,[6] R. Fatemi,[30] S. Fazio,[6] P. Federic,[38] J. Fedorisin,[28] C. J. Feng,[37] Y. Feng,[43] P. Filip,[28] E. Finch,[50] Y. Fisyak,[6] A. Francisco,[62] L. Fulek,[2] C. A. Gagliardi,[53] T. Galatyuk,[15] F. Geurts,[44] A. Gibson,[58] K. Gopal,[23] D. Grosnick,[58] W. Guryn,[6] A. I. Hamad,[29] A. Hamed,[5] J. W. Harris,[62] W. He,[18] X. He,[26] S. Heppelmann,[8] S. Heppelmann,[41] N. Herrmann,[19] E. Hoffman,[20] L. Holub,[14] Y. Hong,[31] S. Horvat,[62] Y. Hu,[18] H. Z. Huang,[9] S. L. Huang,[51] T. Huang,[37] X. Huang,[55] T. J. Humanic,[39] P. Huo,[51] G. Igo,[9] D. Isenhower,[1] W. W. Jacobs,[25] C. Jena,[23] A. Jentsch,[6] Y. JI,[47] J. Jia,[6,51] K. Jiang,[47] S. Jowzaee,[61] X. Ju,[47] E. G. Judd,[7] S. Kabana,[29] M. L. Kabir,[10] S. Kagamaster,[32] D. Kalinkin,[25] K. Kang,[55] D. Kapukchyan,[10] K. Kauder,[6] H. W. Ke,[6] D. Keane,[29] A. Kechechyan,[28] M. Kelsey,[31] Y. V. Khyzhniak,[35] D. P. Kikoła,[60] C. Kim,[10] B. Kimelman,[8] D. Kincses,[16] T. A. Kinghorn,[8] I. Kisel,[17] A. Kiselev,[6] A. Kisiel,[60] M. Kocan,[14] L. Kochenda,[35] L. K. Kosarzewski,[14] L. Kramarik,[14] P. Kravtsov,[35] K. Krueger,[4] N. Kulathunga Mudiyanselage,[20] L. Kumar,[40] R. Kunnawalkam Elayavalli,[61] J. H. Kwasizur,[25] R. Lacey,[51] S. Lan,[11] J. M. Landgraf,[6] J. Lauret,[6] A. Lebedev,[6] R. Lednicky,[28] J. H. Lee,[6] Y. H. Leung,[31] C. Li,[47] W. Li,[49] W. Li,[44] X. Li,[47] Y. Li,[55] Y. Liang,[29] R. Licenik,[38] T. Lin,[53] Y. Lin,[11] M. A. Lisa,[39] F. Liu,[11] H. Liu,[25] P. Liu,[51] P. Liu,[49] T. Liu,[62] X. Liu,[39] Y. Liu,[53] Z. Liu,[47] T. Ljubicic,[6] W. J. Llope,[61] R. S. Longacre,[6] N. S. Lukow,[52] S. Luo,[12] X. Luo,[11] G. L. Ma,[49] L. Ma,[18] R. Ma,[6] Y. G. Ma,[49] N. Magdy,[12] R. Majka,[62] D. Mallick,[36] S. Margetis,[29] C. Markert,[54] H. S. Matis,[31] J. A. Mazer,[45] N. G. Minaev,[42] S. Mioduszewski,[53] B. Mohanty,[36] I. Mooney,[61] Z. Moravcova,[14] D. A. Morozov,[42] M. Nagy,[16] J. D. Nam,[52] Md. Nasim,[22] K. Nayak,[11] D. Neff,[9] J. M. Nelson,[7] D. B. Nemes,[62] M. Nie,[48] G. Nigmatkulov,[35] T. Niida,[56] L. V. Nogach,[42] T. Nonaka,[11] G. Odyniec,[31] A. Ogawa,[6] S. Oh,[62] V. A. Okorokov,[35] B. S. Page,[6] R. Pak,[6] A. Pandav,[36] Y. Panebratsev,[28] B. Pawlik,[2] D. Pawlowska,[60] H. Pei,[11] C. Perkins,[7] L. Pinsky,[20] R. L. Pintér,[16] J. Pluta,[60] J. Porter,[31] M. Posik,[52] N. K. Pruthi,[40] M. Przybycien,[2] J. Putschke,[61] H. Qiu,[26] A. Quintero,[52] S. K. Radhakrishnan,[29] S. Ramachandran,[30] R. L. Ray,[54] R. Reed,[32] H. G. Ritter,[31] J. B. Roberts,[44] O. V. Rogachevskiy,[28] J. L. Romero,[8] L. Ruan,[6] J. Rusnak,[38] N. R. Sahoo,[48] H. Sako,[56] S. Salur,[45] J. Sandweiss,[62] S. Sato,[56] W. B. Schmidke,[6] N. Schmitz,[33] B. R. Schweid,[51] F. Seck,[15] J. Seger,[13] M. Sergeeva,[9] R. Seto,[10] P. Seyboth,[33] N. Shah,[24] E. Shahaliev,[28] P. V. Shanmuganathan,[6] M. Shao,[47] F. Shen,[48] W. Q. Shen,[49] S. S. Shi,[11] Q. Y. Shou,[49] E. P. Sichtermann,[31] R. Sikora,[2] M. Simko,[38] J. Singh,[40] S. Singha,[26] N. Smirnov,[62] W. Solyst,[25] P. Sorensen,[6] H. M. Spinka,[4] B. Srivastava,[43] T. D. S. Stanislaus,[58] M. Stefaniak,[60] D. J. Stewart,[62] M. Strikhanov,[35] B. Stringfellow,[43] A. A. P. Suaide,[46] M. Sumbera,[38] B. Summa,[41] X. M. Sun,[11] Y. Sun,[47] Y. Sun,[21] B. Surrow,[52] D. N. Svirida,[3] P. Szymanski,[60] A. H. Tang,[6] Z. Tang,[47] A. Taranenko,[35] T. Tarnowsky,[34] J. H. Thomas,[31] A. R. Timmins,[20] D. Tlusty,[13] M. Tokarev,[28] C. A. Tomkiel,[32] S. Trentalange,[9] R. E. Tribble,[53] P. Tribedy,[6] S. K. Tripathy,[16] O. D. Tsai,[9] Z. Tu,[6] T. Ullrich,[6] D. G. Underwood,[4] I. Upsal,[48,6] G. Van Buren,[6] J. Vanek,[38] A. N. Vasiliev,[42] I. Vassiliev,[17] F. Videbæk,[6] S. Vokal,[28] S. A. Voloshin,[61] F. Wang,[43] G. Wang,[9] J. S. Wang,[21] P. Wang,[47] Y. Wang,[11] Y. Wang,[55] Z. Wang,[48] J. C. Webb,[6] P. C. Weidenkaff,[19] L. Wen,[9] G. D. Westfall,[34] H. Wieman,[31] S. W. Wissink,[25] R. Witt,[57] Y. Wu,[10] Z. G. Xiao,[55] G. Xie,[31] W. Xie,[43] H. Xu,[21] N. Xu,[31] Q. H. Xu,[48] Y. F. Xu,[49] Y. Xu,[48] Z. Xu,[6] Z. Xu,[9] C. Yang,[48] Q. Yang,[48] S. Yang,[6] Y. Yang,[37] Z. Yang,[11] Z. Ye,[44] Z. Ye,[12] L. Yi,[48] K. Yip,[6] H. Zbroszczyk,[60] W. Zha,[47] D. Zhang,[11] S. Zhang,[47] S. Zhang,[49] X. P. Zhang,[55] Y. Zhang,[47] Z. J. Zhang,[37] Z. Zhang,[6] J. Zhao,[43] C. Zhong,[49] C. Zhou,[49] X. Zhu,[55] Z. Zhu,[48] M. Zurek,[31] and M. Zyzak[17]

(STAR Collaboration)

[1] *Abilene Christian University, Abilene, Texas 79699*

arXiv:1910.14628v1 [nucl-ex] 31 Oct 2019

[2] AGH University of Science and Technology, FPACS, Cracow 30-059, Poland
[3] Alikhanov Institute for Theoretical and Experimental Physics NRC "Kurchatov Institute", Moscow 117218, Russia
[4] Argonne National Laboratory, Argonne, Illinois 60439
[5] American University of Cairo, New Cairo 11835, New Cairo, Egypt
[6] Brookhaven National Laboratory, Upton, New York 11973
[7] University of California, Berkeley, California 94720
[8] University of California, Davis, California 95616
[9] University of California, Los Angeles, California 90095
[10] University of California, Riverside, California 92521
[11] Central China Normal University, Wuhan, Hubei 430079
[12] University of Illinois at Chicago, Chicago, Illinois 60607
[13] Creighton University, Omaha, Nebraska 68178
[14] Czech Technical University in Prague, FNSPE, Prague 115 19, Czech Republic
[15] Technische Universität Darmstadt, Darmstadt 64289, Germany
[16] ELTE Eötvös Loránd University, Budapest, Hungary H-1117
[17] Frankfurt Institute for Advanced Studies FIAS, Frankfurt 60438, Germany
[18] Fudan University, Shanghai, 200433
[19] University of Heidelberg, Heidelberg 69120, Germany
[20] University of Houston, Houston, Texas 77204
[21] Huzhou University, Huzhou, Zhejiang 313000
[22] Indian Institute of Science Education and Research (IISER), Berhampur 760010 , India
[23] Indian Institute of Science Education and Research (IISER) Tirupati, Tirupati 517507, India
[24] Indian Institute Technology, Patna, Bihar 801106, India
[25] Indiana University, Bloomington, Indiana 47408
[26] Institute of Modern Physics, Chinese Academy of Sciences, Lanzhou, Gansu 730000
[27] University of Jammu, Jammu 180001, India
[28] Joint Institute for Nuclear Research, Dubna 141 980, Russia
[29] Kent State University, Kent, Ohio 44242
[30] University of Kentucky, Lexington, Kentucky 40506-0055
[31] Lawrence Berkeley National Laboratory, Berkeley, California 94720
[32] Lehigh University, Bethlehem, Pennsylvania 18015
[33] Max-Planck-Institut für Physik, Munich 80805, Germany
[34] Michigan State University, East Lansing, Michigan 48824
[35] National Research Nuclear University MEPhI, Moscow 115409, Russia
[36] National Institute of Science Education and Research, HBNI, Jatni 752050, India
[37] National Cheng Kung University, Tainan 70101
[38] Nuclear Physics Institute of the CAS, Rez 250 68, Czech Republic
[39] Ohio State University, Columbus, Ohio 43210
[40] Panjab University, Chandigarh 160014, India
[41] Pennsylvania State University, University Park, Pennsylvania 16802
[42] NRC "Kurchatov Institute", Institute of High Energy Physics, Protvino 142281, Russia
[43] Purdue University, West Lafayette, Indiana 47907
[44] Rice University, Houston, Texas 77251
[45] Rutgers University, Piscataway, New Jersey 08854
[46] Universidade de São Paulo, São Paulo, Brazil 05314-970
[47] University of Science and Technology of China, Hefei, Anhui 230026
[48] Shandong University, Qingdao, Shandong 266237
[49] Shanghai Institute of Applied Physics, Chinese Academy of Sciences, Shanghai 201800
[50] Southern Connecticut State University, New Haven, Connecticut 06515
[51] State University of New York, Stony Brook, New York 11794
[52] Temple University, Philadelphia, Pennsylvania 19122
[53] Texas A&M University, College Station, Texas 77843
[54] University of Texas, Austin, Texas 78712
[55] Tsinghua University, Beijing 100084
[56] University of Tsukuba, Tsukuba, Ibaraki 305-8571, Japan
[57] United States Naval Academy, Annapolis, Maryland 21402
[58] Valparaiso University, Valparaiso, Indiana 46383
[59] Variable Energy Cyclotron Centre, Kolkata 700064, India
[60] Warsaw University of Technology, Warsaw 00-661, Poland
[61] Wayne State University, Detroit, Michigan 48201
[62] Yale University, New Haven, Connecticut 06520

(Dated: November 1, 2019)

We report on the first measurement of the charmed baryon $\Lambda_c^{\pm}$ production at midrapidity ($|y|<1$) in Au+Au collisions at $\sqrt{s_{\rm NN}} = 200$ GeV collected by the STAR experiment at the Relativistic Heavy Ion Collider. The Λ_c/D^0 (denoting $(\Lambda_c^+ + \Lambda_c^-)/(D^0 + \overline{D}^0)$) yield ratio is measured to be 1.08 ± 0.16 (stat.) ± 0.26 (sys.) in the 0–20% most central Au+Au collisions for the transverse momentum (p_T) range $3 < p_T < 6$ GeV/c. This is significantly larger than the PYTHIA model calculations for $p+p$ collisions. The measured Λ_c/D^0 ratio, as a function of p_T and collision centrality, is comparable to the baryon-to-meson ratios for light and strange hadrons in Au+Au collisions. Model calculations including coalescence hadronization for charmed baryon and meson formation reproduce the features of our measured Λ_c/D^0 ratio.

Heavy ion collisions offer a unique opportunity to study Quantum Chromodynamics (QCD), the theory describing strong interactions between quarks and gluons through color charges. Data collected from the Relativistic Heavy Ion Collider (RHIC) and the Large Hadron Collider (LHC) demonstrate that a novel QCD matter, Quark-Gluon Plasma (QGP), in which quarks and gluons are deconfined, is created in high-energy nucleus-nucleus collisions [1, 2]. Measurements of the abundance ratios of various hadrons in heavy-ion collisions and their modifications with respect to those in p+p, e^++e^- and e^-+p collisions can provide insights into the mechanism by which hadrons are formed from the deconfined QGP phase.

QCD hadronization is a nonperturbative process and to this date remains a challenging process to model. A fragmentation hadronization scheme has been widely tested and accepted for high-momentum transfer processes. Fragmentation schemes encounter challenges in trying to explain the enhancement in baryon-to-meson ratios for light hadrons in the transverse momentum (p_T) region of $2 < p_T < 6$ GeV/c in heavy-ion collisions [3–5]. A coalescence hadronization mechanism, in which hadrons can be formed via recombination of close-by partons in phase space, has been deployed to reproduce this enhancement [6, 7]. Alternatively to these microscopic schemes, a statistical hadronization scheme has been used to fit successfully various light and strange hadron integrated yields in both heavy-ion and more elementary collisions [8].

Due to their large masses, heavy quarks (c, b) are predominately created from initial hard scatterings in heavy-ion collisions. The relative yields of heavy-flavor hadrons can serve as a tool to study their hadronization process. The c quark fragmentation fraction ratio $(c \to \Lambda_c^+)/(c \to D^0)$ has been measured to be around 0.10–0.15 in $e^+ + e^-$ and $e^- + p$ collisions [9–11]. These measured fragmentation fractions have been widely used in QCD calculations for charm hadron production. Recently, ALICE and LHCb measured [12, 13] the Λ_c/D^0 ratio in $p + p$ and p + Pb collisions at the LHC to be 0.4–0.5 at $2 < p_T < 8$ GeV/c, larger than the PYTHIA model [14] calculation based on Lund string fragmentation. PYTHIA model with color reconnection [15] and DIPSY model with rope hadronization [16] can enhance the Λ_c/D^0 ratio in this $p_{\rm T}$ region, but still cannot reproduce the data quantitatively.

In heavy-ion collisions, models including coalescence hadronization of charm quarks predict a large Λ_c/D^0 ratio of $\sim$1, in the low to intermediate p_T regions ($<\sim$ 8 GeV/c) [17–19]. The ALICE Collaboration reported the Λ_c/D^0 ratio to be $\sim$1 at $6 < p_T < 12$ GeV/c in Pb+Pb collisions at $\sqrt{s_{\rm NN}} = 5.02$ TeV, conceivable with a contribution of coalescence hadronization for charm quarks [20]. Measurement of $\Lambda_c^{\pm}$ production over a broad momentum region, particularly at lower p_T, will offer significant insights into the hadronization mechanism of heavy quarks in the presence of QGP. Furthermore, understanding the hadronization mechanism of charm quarks in heavy-ion collisions is crucial to the interpretation of the nuclear modification factor and elliptic flow data of D mesons [21–23] and electrons from heavy-flavor hadron decays [24, 25] in heavy-ion collisions.

In this Letter, we report on the first measurement of $\Lambda_c^{\pm}$ production in Au+Au collisions at $\sqrt{s_{\rm NN}} = 200$ GeV. The analysis is carried out at midrapidity ($|y|<1$), and utilized a total of 2.3 billion minimum bias (MB) triggered events collected by the STAR experiment during 2014 and 2016 runs at RHIC. The Heavy Flavor Tracker (HFT) [26], a high resolution silicon detector system, was installed at STAR during these runs. The HFT consists of four sub-detectors, two layers of Pixel detectors (PXL) closest to the beam pipe, the Intermediate Silicon Tracker (IST) outside the PXL layers, and the Silicon Strip Detector (SSD) as the outermost layer. The excellent vertex position resolution provided by the HFT significantly improved the signal-to-background ratio for charmed hadron reconstruction. The MB events are selected by requiring a coincidence between the east and west Vertex Position Detectors (VPD) [27], and are also required to have the reconstructed primary vertex position along the beam direction within 6 cm from the detector center, to ensure good HFT acceptance. The collision centrality, a measure of the geometric overlap between the two colliding nuclei, is defined using the measured charged track multiplicity at mid-rapidity, as compared to a Monte Carlo Glauber simulation [28].

The $\Lambda_c^{\pm}$ baryons are reconstructed via the hadronic decay channel $\Lambda_c^+ \to K^-\pi^+p$ and its charge conjugate. Charged particle tracks are reconstructed from hits in the STAR Time Projection Chamber (TPC) [29] and HFT detectors, in a 0.5 T magnetic field. Tracks are

required to have a minimum of 20 TPC hits (out of a maximum of 45) and at least three hits in the HFT sub-detectors with two of them in the two PXL layers. The tracks are also required to be within pseudorapidity $|\eta| < 1$ with $p_T > 0.5\,\mathrm{GeV}/c$ and their distance of closest approach (DCA) from the primary vertex to be within 1.5 cm. Particle identification (PID) is achieved by requiring the ionization energy loss, dE/dx, measured by the TPC to be within three standard deviations from the expected values for π and to be within two standard deviations for K and p. The particle identification is further extended up to $p_T \sim 3\,\mathrm{GeV}/c$ by the Time Of Flight (TOF) detector [30], by requiring $1/\beta$ (β is the particle velocity in the unit of speed of light), calculated from the path length and measured time of flight, to be within three standard deviations from the expected values.

The $\Lambda_c^{\pm}$ decay vertex is reconstructed as the mid-point of the DCA between the $K\pi p$ tracks. The combinatorial background from random combinations of $K\pi p$ tracks originating from the primary vertex is large, as the $\Lambda_c^{\pm}$ decay length is rather short ($c\tau = 60\,\mu$m) [31]. To improve the separation of signal from background, we have used a supervised machine learning algorithm, the Boosted Decision Trees (BDT), implemented in the TMVA package [32]. The BDTs are trained with a signal sample of $\Lambda_c^{\pm} \to K\pi p$ decays simulated using the EvtGen generator [33] with detector effects taken into account and a background sample of wrong-sign combinations of $K\pi p$ triplets from a subset of the data. The cut on BDT response is optimized for maximum $\Lambda_c^{\pm}$ signal significance using the estimated number of signal and background $\Lambda_c^{\pm}$ candidates in the data. Figure 1 shows examples of the invariant mass distributions with the BDT selection, of the $K\pi p$ triplets with the right and wrong-sign (scaled by 1/3) combinations. The distributions in the 0–20% most central collisions (top) and the 10–80% central collisions (bottom), the centrality range used for p_T dependent measurement, are shown. The right-sign distributions are fit to a Gaussian for the signal plus a second order polynomial for the background, with the shape of the polynomial function fixed from fitting to the wrong-sign distribution. Correlated background can also contribute to right-sign distributions. While the overall normalization of the background is found to differ between the right-sign and wrong-sign distributions, the shapes of the two distributions are statistically indistinguishable. The raw signal yields are obtained as the counts of the right-sign triplets within an invariant mass window of three standard deviations of the Gaussian fit to the mass peak with counts from background, evaluated using the polynomial component of the fit, in the same mass window subtracted.

The $\Lambda_c^{\pm}$ reconstruction efficiency is evaluated using a hybrid method, similarly to the D^0 spectra measurement with the STAR HFT [21]. The TPC tracking efficiency is obtained using the standard embedding technique used

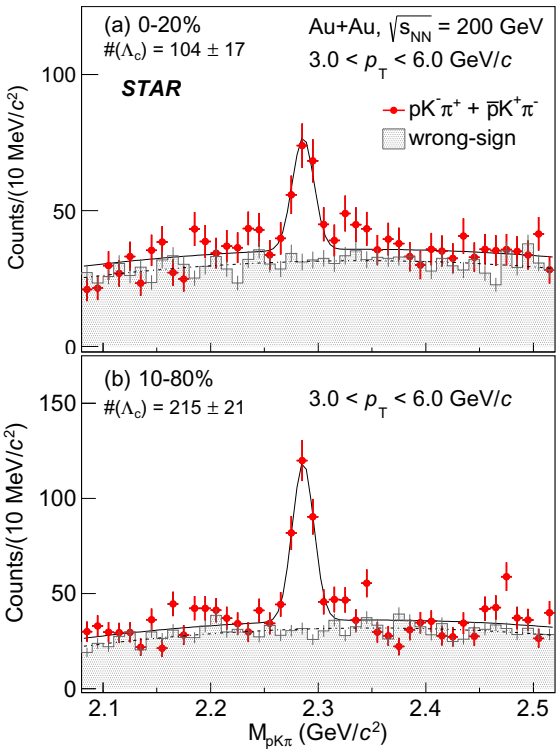

FIG. 1. The $pK\pi$ invariant mass distributions for right-sign (solid red data points) and wrong-sign (shaded histograms) combinations in Au+Au collisions at $\sqrt{s_{\mathrm{NN}}} = 200\,\mathrm{GeV}$ for 0–20% (top) and 10–80% (bottom) centrality classes. The wrong-sign distributions are scaled by 1/3, the ratio of number of right-sign to wrong-sign combinations for the $pK\pi$ triplet. The error bars shown are statistical uncertainties. The solid line depicts a fit with a Gaussian function, for $\Lambda_c^{\pm}$ signal, and a second order polynomial function, the shape of which is fixed by fit to the wrong-sign distribution (dashed line), for the background.

widely in many other STAR analyses. The PID efficiencies are evaluated using pure π, K, p samples from data. The HFT tracking and the BDT selection efficiency are calculated using a data-driven simulation framework with the input distributions taken from the real data. The input distributions include the TPC-to-HFT matching efficiency (the fraction of good TPC tracks matched to hits in HFT) and the DCA distributions of tracks with respect to the reconstructed collision vertex. Protons reconstructed in the real data have a sizable secondary contribution from other hyperon decays, which impacts the TPC-to-HFT matching ratio and DCA distributions. A correction factor to the efficiency calculated using the data-driven simulation is evaluated using Au+Au events from HIJING [34] propagated through the STAR GEANT detector geometry [35] and embedded into zero-bias data (denoted HIJING+ZB). Zero-bias data consist of events taken with no trigger requirement, and capture the background conditions in the detectors during

the run. The $p_{\rm T}$ distributions of protons and hyperons from HIJING are reweighted to match the distributions in data [3, 36]. The events are then reconstructed with the same reconstruction algorithm as the real data. The correction is calculated as a ratio of the efficiency from the data-driven simulation, using the input distributions for inclusive tracks from the reconstructed HIJING+ZB data, to the one using inputs from primary tracks from the same data. The correction factor is found to be about 30% with very weak p_T and centrality dependences. The impact of the finite primary vertex resolution on the reconstruction efficiency obtained by this method is also evaluated using the HIJING+ZB events with procedures similar to those described in [21]. It is found to be within 10% for the 50–80% peripheral centrality class and negligible for the other more central events. The yields are finally corrected for the $\Lambda_c^{\pm} \rightarrow K\pi p$ branching ratio (B.R.) of 6.28 ± 0.32% [31].

The systematic uncertainties to the measurement include the uncertainties in raw yield extraction and various efficiency correction factors. The former is evaluated by varying the background estimation method (varying the fit range, choice of background function and leaving the background shape unconstrained), and is between 6–14% in the measured p_T region. The contribution to the yield under the mass peak from incorrectly assigned PID for daughter tracks is less than 1%. The TPC efficiency uncertainty is evaluated to be ∼15%, and PID efficiency uncertainties to be ∼6%, for three daughter tracks combined. The uncertainty in the HFT tracking and topological cut efficiency is estimated by changing the BDT response cuts so that the reconstruction efficiency varies by 50% above and below the nominal one. The resulting non-statistical variations to final results are included in the systematic uncertainties and range from 10–15%. For the correction factor due to secondary protons, the uncertainties from the measured proton and Λ spectra [3, 36], as well as those on other hadrons that decay to protons, are propagated. This uncertainty is estimated to be about 4%. We also include a 10% uncertainty from a closure test for the data-driven simulation method, evaluated by comparing the efficiencies calculated using data-driven simulation with input distributions from reconstructed HIJING+ZB events, to the efficiencies evaluated directly from the reconstructed HIJING+ZB events. The feed-down contribution from bottom hadrons to the measurements is found to be small and less than 4% in the measured p_T range. Finally, the uncertainty in the decay B.R. from the latest PDG [31] value is added as a global normalization uncertainty in the $\Lambda_c^{\pm}$ yield.

The $\Lambda_c^{\pm}$ invariant yields in the 10-80% centrality class for the different $p_{\rm T}$ bins used in the analysis are shown in Table I, along with the statistical and systematic uncertainties. The 10-80% centrality class is chosen for $p_{\rm T}$ dependent measurement as it had the best Λ_c signal significance in the measured regions. The ratio of the invariant yield of $\Lambda_c^{\pm}$ to that of D^0 is shown as a function of p_T in Fig. 2 for the 10–80% centrality class. The correlated systematic uncertainties from the efficiency correction that go into both the $\Lambda_c^{\pm}$ and the D^0 measurements, cancel. Figure 2 (a) compares the Λ_c/D^0 ratio to the baryon-to-meson ratios from light and strange flavor hadrons [3, 36]. The Λ_c/D^0 ratio is comparable in magnitude to the Λ/K_s^0 and p/π ratios and shows a similar p_T dependence in the measured region.

$p_{\rm T}$ (GeV/c)	$1/(2\pi p_{\rm T} N_{\rm evt}) {\rm d}^2N/{\rm d}p_{\rm T}{\rm d}y$ (GeV/c)$^{-2}$
2.5 - 3.5	$8.2\times10^{-4}\pm 1.4\times10^{-4}$ (stat.) $\pm 2.4\times10^{-4}$ (sys.)
3.5 - 5.0	$6.0\times10^{-5}\pm 7.7\times10^{-6}$ (stat.) $\pm 1.5\times10^{-5}$ (sys.)
5.0 - 8.0	$2.1\times10^{-6}\pm 3.8\times10^{-7}$ (stat.) $\pm 5.5\times10^{-7}$ (sys.)

TABLE I. The $\Lambda_c^{\pm}$ invariant yields measured in the 10-80% centrality class for the different $p_{\rm T}$ bins, in Au+Au collisions at $\sqrt{s_{\rm NN}}$= 200 GeV.

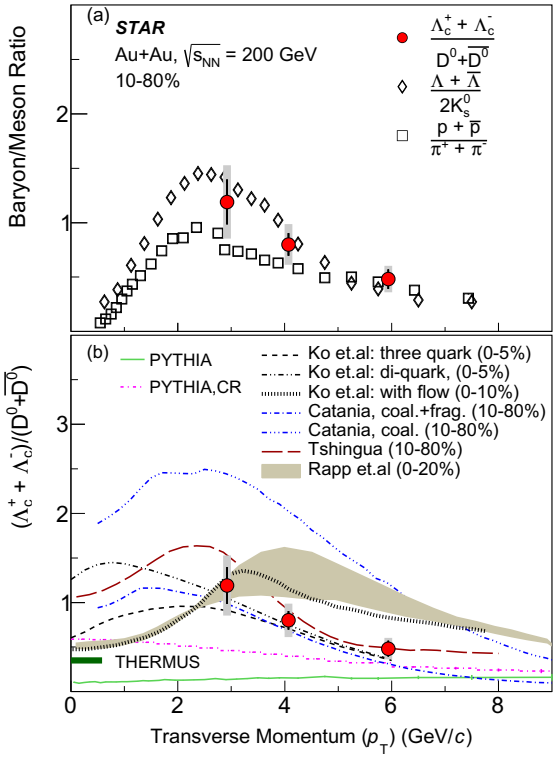

FIG. 2. The measured Λ_c/D^0 ratio at midrapidity ($|y| < 1$) as a function of $p_{\rm T}$ for Au+Au collisions at $\sqrt{s_{\rm NN}} = 200\,{\rm GeV}$ in 10-80% centrality, compared to the baryon-to-meson ratios for light and strange hadrons (top) and various model calculations (bottom). The vertical lines and shaded boxes on the Λ_c/D^0 data points indicate statistical and systematic uncertainties respectively. The $p_{\rm T}$ integrated Λ_c/D^0 ratio from the THERMUS [8] model calculation with a freeze-out temperature of $T_{\rm ch} = 160\,{\rm MeV}$ is shown as a horizontal bar on the left axis of the plot.

The measured values are compared to different model

calculations for the Λ_c/D^0 ratio in panel (b) of Fig. 2. The values show a significant enhancement compared to the calculations from the latest PYTHIA 8.24 release (Monash tune [37]) without color reconnections (CR) [15]. The implementation with CR (CR mode2 in [15]) is found to enhance the baryon production with respect to mesons. However, both calculations fail to fully describe the data and its p_T dependence. The mode without CR is ruled out at a p-value of 1 $\times 10^{-4}$ (χ^2/NDF = 20.7/3), while the CR mode gives a p-value of 0.04 (χ^2/NDF = 8.2/3) using a reduced χ^2 test. The measured Λ_c/D^0 yield ratio in Au+Au collisions at $\sqrt{s_{\rm NN}}$ = 200 GeV is also larger compared to those measured in p+p and p+Pb collisions at the LHC [12, 38].

The enhanced baryon-to-meson ratio for the light- and strange-flavor hadrons and their p_T dependence is usually attributed to the coalescence hadronization of partons inside the QGP. Figure 2 (b) also shows the comparison to various models with coalescence hadronization of charm quarks. The Catania model [39] and the model from Ko et al. with three quarks [17] use a similar framework for coalescence with differing values for the heavy hadron radii and distributions of quarks in the QGP. The model from Ko et al. with di-quarks allows for the presence of bound di-quark domains in the medium which can further enhance the baryon production. The calculations from Ko et al. [40] with flow is a recent update that takes into account the mass dependence of collective flow of hadrons observed in heavy-ion collisions. The Tsinghua model [41] uses a sequential coalescence hadronization of charm quarks together with charm quark conservation. The model from Rapp et al. [42] also utilizes a coalescence hadronization framework, with an equilibrium limit that takes into account the feed-down contributions from higher mass charm baryon states predicted by lattice QCD calculations. These models are able to give enhanced Λ_c/D^0 yield ratios and describe the measured ratio around $p_{\rm T}$ = 3 GeV/c. A reduced χ^2 test is carried out with the coalescence model calculations, taking into account the finite $p_{\rm T}$ bin-width in the measurement. The Catania model calculations of the Λ_c/D^0 ratio from hadrons formed only through coalescence hadronization over-predicts the measurement at all $p_{\rm T}$ (reduced χ^2 = 26.1). The calculations from Ko et al. with flow and from Rapp et al. give reduced χ^2 values of 4.8 and 5.9 respectively, from the over-prediction of the ratio in the highest two $p_{\rm T}$ bins. The other coalescence model calculations are consistent with data within uncertainties over the measured $p_{\rm T}$ range, with reduced χ^2 values $<$ 1. It should be noted that the calculations from Rapp et al. and Ko et al. have centrality ranges that differ from those in the measurement, which may impact the χ^2 values quoted. In the models discussed above, D^0 meson radial flow is implicitly included mainly through the charm quark diffusion in the medium. However, it was found that a purely radial flow effect, evaluated using a Blast-Wave model with freeze-out parameters from D^0 measurement [21], causes the Λ_c/D^0 ratio to rise strongly with increaseing p_T in the measured p_T region. This is similar to the behavior observed for light hadrons [4], and opposite to the trend measured in the data. The comparisons suggest coalescence hadronization plays an important role in charm-quark hadronization in the presence of QGP. Also, the data can be used to constrain the coalescence model calculations and their model parameters.

The $\Lambda_c^{\pm}$ production cross section per nucleon-nucleon collision, $d\sigma/dy|_{y=0}$, for 10–80% Au+Au collisions at 200 GeV is determined to be 34 $\pm$ 5 (stat) $\pm$ 9 (sys,data) $\pm$ 17 (sys,model) μb by extrapolating the measured yields to p_T = 0 GeV/c using fits with the different coalescence model calculations shown in 2(b). The mean of the extrapolated values from different models is taken as the central value and the maximum difference between them is included in the systematic uncertainty, along with the systematic uncertainties propagated from data. The p_T-integrated Λ_c/D^0 ratio is 0.82 $\pm$ 0.12 (stat) $\pm$ 0.22 (sys,data) $\pm$ 0.41 (sys,model). This is higher, but consistent including extrapolation uncertainties, to the value (0.35) from thermal model calculation using THERMUS [8] with a freeze-out temperature, $T_{\rm ch}$ = 160 MeV. This suggests $\Lambda_c^{\pm}$ may contribute sizably to the total charm yield in heavy-ion collisions.

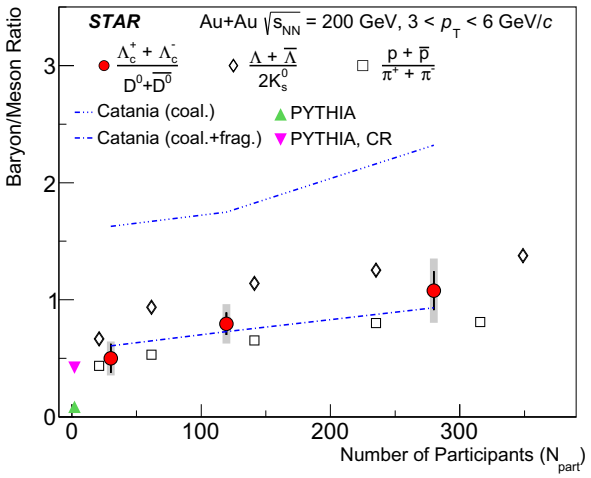

FIG. 3. The measured Λ_c/D^0 yield ratio in $3 < p_{\rm T} < 6$ GeV/c (solid circles) as a function of collision centrality (expressed in $N_{\rm part}$) for Au+Au collisions at $\sqrt{s_{\rm NN}}$ = 200 GeV. The open diamonds and squares show the baryon-to-meson ratio measured for strange and light-flavor hadrons respectively. The vertical lines and the shaded boxes on the Λ_c/D^0 data points indicate statistical and systematic uncertainties respectively. The dashed curves indicate the Λ_c/D^0 ratio calculated from a model with charm quark coalescence, and the up and down triangles indicate the ratios from the PYTHIA model for p+p collisions without and with color reconnection (CR) respectively, for the same $p_{\rm T}$ region.

The centrality dependence of the Λ_c/D^0 ratio, plotted as function of the number of participant nucleons $N_{\rm part}$, for $3 < p_T < 6$ GeV/c is shown in Fig. 3. The measurements correspond to the centrality ranges 50-80%, 20-50% and 0-20%. The Λ_c/D^0 ratio shows an increase towards more central collisions. The increasing trend is qualitatively similar to that seen for the baryon-to-meson ratio for light and strange-flavor hadrons, and to that predicted by coalescence model calculations. The measured Λ_c/D^0 ratio in 0-20% central collisions of 1.08 $\pm$ 0.16(stat.) $\pm$ 0.26(sys.) is larger than the values from PYTHIA 8.2 without CR (at 3.1 σ significance) and with CR (at 2.1 σ significance).

In summary, STAR reports on the first measurement of $\Lambda_c^{\pm}$ baryon production in Au+Au collisions at $\sqrt{s_{\rm NN}} =$ 200 GeV utilizing its high-resolution silicon detector. The measured Λ_c/D^0 yield ratio at midrapidity ($|y| < 1$) is found to be comparable to the baryon-to-meson ratios for light and strange-flavor hadrons in the same kinematic regions. The large Λ_c/D^0 ratio also suggests that charmed baryons contribute significantly to the total charm cross section at midrapidity in heavy-ion collisions at RHIC. The Λ_c/D^0 ratio in Au+Au collisions is considerably larger than the PYTHIA expectation at the same energy. Several model calculations that include coalescence hadronization for charm hadron formation can reproduce the features of our data, suggesting coalescence plays an important role in charm quark hadronization in heavy-ion collisions in the measured $p_{\rm T}$ regions.

We thank the RHIC Operations Group and RCF at BNL, the NERSC Center at LBNL, and the Open Science Grid consortium for providing resources and support. This work was supported in part by the Office of Nuclear Physics within the U.S. DOE Office of Science, the U.S. National Science Foundation, the Ministry of Education and Science of the Russian Federation, National Natural Science Foundation of China, Chinese Academy of Science, the Ministry of Science and Technology of China and the Chinese Ministry of Education, the National Research Foundation of Korea, Czech Science Foundation and Ministry of Education, Youth and Sports of the Czech Republic, Hungarian National Research, Development and Innovation Office, New National Excellency Programme of the Hungarian Ministry of Human Capacities, Department of Atomic Energy and Department of Science and Technology of the Government of India, the National Science Centre of Poland, the Ministry of Science, Education and Sports of the Republic of Croatia, RosAtom of Russia and German Bundesministerium fur Bildung, Wissenschaft, Forschung and Technologie (BMBF) and the Helmholtz Association.

[1] Y. Akiba *et al.*, (2015), arXiv:1502.02730 [nucl-ex].

[2] J. Adams *et al.* (STAR), Nucl. Phys. **A757**, 102 (2005), arXiv:nucl-ex/0501009 [nucl-ex]; K. Adcox *et al.* (PHENIX), Nucl. Phys. **A757**, 184 (2005), arXiv:nucl-ex/0410003 [nucl-ex]; B. B. Back *et al.*, Nucl. Phys. **A757**, 28 (2005), arXiv:nucl-ex/0410022 [nucl-ex]; I. Arsene *et al.* (BRAHMS), Nucl. Phys. **A757**, 1 (2005), arXiv:nucl-ex/0410020 [nucl-ex].

[3] B. I. Abelev *et al.* (STAR), Phys. Rev. Lett. **97**, 152301 (2006), arXiv:nucl-ex/0606003 [nucl-ex].

[4] B. B. Abelev *et al.* (ALICE), Phys. Rev. Lett. **111**, 222301 (2013), arXiv:1307.5530 [nucl-ex].

[5] B. I. Abelev *et al.* (STAR), Phys. Lett. **B655**, 104 (2007), arXiv:nucl-ex/0703040 [nucl-ex].

[6] Z.-w. Lin and D. Molnar, Phys. Rev. **C68**, 044901 (2003), arXiv:nucl-th/0304045 [nucl-th].

[7] R. J. Fries, V. Greco, and P. Sorensen, Ann. Rev. Nucl. Part. Sci. **58**, 177 (2008), arXiv:0807.4939 [nucl-th].

[8] S. Wheaton, J. Cleymans, and M. Hauer, Comput. Phys. Commun. **180**, 84 (2009), arXiv:hep-ph/0407174 [hep-ph].

[9] R. Barate *et al.* (ALEPH), Eur. Phys. J. **C16**, 597 (2000), arXiv:hep-ex/9909032 [hep-ex].

[10] H. Abramowicz *et al.* (ZEUS), JHEP **09**, 058 (2013), arXiv:1306.4862 [hep-ex].

[11] M. Lisovyi, A. Verbytskyi, and O. Zenaiev, EPJ Web Conf. **120**, 03002 (2016).

[12] S. Acharya *et al.* (ALICE), JHEP **04**, 108 (2018), arXiv:1712.09581 [nucl-ex].

[13] R. Aaij *et al.* (LHCb), JHEP **02**, 102 (2019), arXiv:1809.01404 [hep-ex].

[14] T. Sjostrand, S. Mrenna, and P. Z. Skands, JHEP **05**, 026 (2006), arXiv:hep-ph/0603175 [hep-ph].

[15] C. Bierlich and J. R. Christiansen, Phys. Rev. **D92**, 094010 (2015), arXiv:1507.02091 [hep-ph].

[16] C. Bierlich, G. Gustafson, L. Lonnblad, and A. Tarasov, JHEP **03**, 148 (2015), arXiv:1412.6259 [hep-ph].

[17] Y. Oh, C. M. Ko, S. H. Lee, and S. Yasui, Phys. Rev. **C79**, 044905 (2009), arXiv:0901.1382 [nucl-th].

[18] V. Greco, C. M. Ko, and R. Rapp, Phys. Lett. **B595**, 202 (2004), arXiv:nucl-th/0312100 [nucl-th].

[19] S. H. Lee, K. Ohnishi, S. Yasui, I.-K. Yoo, and C.-M. Ko, Phys. Rev. Lett. **100**, 222301 (2008), arXiv:0709.3637 [nucl-th].

[20] S. Acharya *et al.* (ALICE), Phys. Lett. **B793**, 212 (2019), arXiv:1809.10922 [nucl-ex].

[21] J. Adam *et al.* (STAR), Phys. Rev. **C99**, 034908 (2019), arXiv:1812.10224 [nucl-ex].

[22] A. M. Sirunyan *et al.* (CMS), Phys. Lett. **B782**, 474 (2018), arXiv:1708.04962 [nucl-ex].

[23] J. Adam *et al.* (ALICE), JHEP **03**, 081 (2016), arXiv:1509.06888 [nucl-ex].

[24] A. Adare *et al.* (PHENIX),

Phys. Rev. Lett. **98**, 172301 (2007), arXiv:nucl-ex/0611018 [nucl-ex].
[25] B. I. Abelev *et al.* (STAR), Phys. Rev. Lett. **98**, 192301 (2007), [Erratum: Phys. Rev. Lett.106,159902(2011)], arXiv:nucl-ex/0607012 [nucl-ex].
[26] G. Contin *et al.*, Nucl. Instrum. Meth. **A907**, 60 (2018), arXiv:1710.02176 [physics.ins-det].
[27] W. J. Llope *et al.*, Nucl. Instrum. Meth. **A522**, 252 (2004), arXiv:nucl-ex/0308022 [nucl-ex].
[28] B. I. Abelev *et al.* (STAR), Phys. Rev. **C79**, 034909 (2009), arXiv:0808.2041 [nucl-ex].
[29] M. Anderson *et al.*, Nucl. Instrum. Meth. **A499**, 659 (2003), arXiv:nucl-ex/0301015 [nucl-ex].
[30] W. J. Llope (STAR), Nucl. Instrum. Meth. **A661**, S110 (2012).
[31] M. Tanabashi *et al.* (Particle Data Group), Phys. Rev. **D98**, 030001 (2018).
[32] A. Hoecker *et al.*, (2007), arXiv:physics/0703039 [physics.data-an].
[33] D. J. Lange, Nucl. Instrum. Meth. **A462**, 152 (2001).
[34] M. Gyulassy and X.-N. Wang, Comput. Phys. Commun. **83**, 307 (1994), arXiv:nucl-th/9502021 [nucl-th].
[35] S. Agostinelli *et al.* (GEANT4), Nucl. Instrum. Meth. **A506**, 250 (2003).
[36] G. Agakishiev *et al.* (STAR), Phys. Rev. Lett. **108**, 072301 (2012), arXiv:1107.2955 [nucl-ex].
[37] P. Skands, S. Carrazza, and J. Rojo, Eur. Phys. J. **C74**, 3024 (2014), arXiv:1404.5630 [hep-ph].
[38] Aaij, R. and others (LHCb), (2018), arXiv:1809.01404 [nucl-ex].
[39] S. Plumari, V. Minissale, S. K. Das, G. Coci, and V. Greco, Eur. Phys. J. **C78**, 348 (2018), arXiv:1712.00730 [hep-ph].
[40] S. Cho, K.-J. Sun, C. M. Ko, S. H. Lee, and Y. Oh, (2019), arXiv:1905.09774 [nucl-th].
[41] J. Zhao, S. Shi, N. Xu, and P. Zhuang, (2018), arXiv:1805.10858 [hep-ph].
[42] M. He and R. Rapp, (2019), arXiv:1905.09216 [nucl-th].